

# OH emission and absorption associated with supernovae in Arp 220

Colin J. Lonsdale<sup>1</sup>, Katherine R. de Kleer<sup>1</sup>, Philip J. Diamond<sup>2</sup>,  
Hannah Thrall<sup>2</sup>, Carol J. Lonsdale<sup>3</sup> and Harding E. Smith<sup>4</sup>

<sup>1</sup>MIT Haystack Observatory, Westford, MA 01886

<sup>2</sup>Jodrell Bank Observatory, Macclesfield, SK11 9DL, UK

<sup>3</sup>Infrared Processing and Analysis Center, MS 100-22, Pasadena, CA 91125, USA

<sup>4</sup>CASS, U.C. San Diego, 9500 Gilman Dr., La Jolla CA 92093-0424, USA

**Abstract.** We present parsec-resolution spectral-line VLBI data for two epochs separated by 15 months as a precise new probe of the innermost regions of the nearby Ultraluminous Infrared Galaxy (ULIRG) Arp 220. This galaxy hosts a powerful starburst, with an associated supernova (SN) rate of order 4/yr. An extensive population of compact continuum sources interpreted as radio supernovae (RSNe) and young supernova remnants (SNR) has been imaged. We show here that many of the supernova-related radio continuum point sources exhibit clear evidence of OH absorption or maser emission in the intervening gas, and as such provide us with a sampling of conditions along very narrow and specific lines of sight through the nuclear environment. The OH gas along these lines of sight exhibits velocity dispersions of up to several tens of km/sec, and that in some cases, multiple distinct concentrations of masing gas at different radial velocities can be discerned. There is evidence for variability in the OH properties on  $\sim 1$ yr timescales. Our results are discussed in the context of the overall OH megamaser properties of Arp 220.

**Keywords.** galaxies: active — infrared: galaxies — radio lines: galaxies — masers

---

## 1. Introduction

The galaxy Arp 220 (IC 4553) is the closest Ultraluminous Infrared galaxy (ULIRG), and has consequently been the subject of intense multi-wavelength study. A persistent challenge for all these studies, however, is the fact that the source of the extreme luminosity of the system lies deep in the innermost regions of the twin galaxy nuclei, where optical depths are extreme. To overcome this problem, we have therefore been exploiting the technique of Very Long Baseline Interferometry (VLBI) to probe the nuclei of Arp 220 with parsec-scale linear resolution. Such studies have revealed clusters of weak continuum point sources identified as radio supernovae (RSNe) and young supernova remnants (SNR), tracing a powerful ongoing nuclear starburst (Smith *et al.* 1998, Rovilos *et al.* 2005, Parra *et al.*, 2007). Lonsdale *et al.* (2006) catalogued 49 continuum sources, including 4 new sources in a 12-month interval.

Arp 220 is also a powerful OH megamaser galaxy, and indeed the megamaser phenomenon was originally discovered by Baan, Wood and Haschick (1982) in this galaxy. A series of VLBI studies capable of spatially resolving the emission has shown the presence of considerable variety in the properties of different maser components in the source (Diamond *et al.* 1989, Lonsdale *et al.* 1998, Rovilos *et al.* 2003). In particular there are now known to be two observationally distinct components of the maser emission, one that is diffuse on  $\sim 100$ pc scales and exhibits relatively modest 1667MHz/1665MHz line ratios, and a second that appears on much smaller size scales ( $< 1$  to 10 pc) and features extremely high 1667MHz/1665MHz line ratios.

These observations prompted speculation that diffuse and compact maser components arise in gas clouds with physically different properties. The diffuse component was thought to arise in a screen of OH clouds, each supporting low-gain unsaturated masing, while the compact component, which exhibits relatively high gain, was hypothesized to originate in physically small clouds, presenting a challenge to radiative pumping models driven by the far infrared radiation field of the galaxy nucleus. More recently, and based substantially on VLBI observations of another OH megamaser galaxy IIZw35 (Diamond *et al.* 1999, Pihlström *et al.* 2001), an alternative explanation for compact, bright OH megamaser components has been explored (Parra *et al.* 2005). In this interpretation, only one class of OH cloud exists, and compact features arise due to chance superposition of multiple such clouds along our line of sight.

Consideration of this model demonstrates that in a clumpy medium the effects of cloud superposition along our line of sight can be significant, and must be accounted for in any complete megamaser model. The cloud overlap model of Parra *et al.* (2005) succeeds in IIZw35, primarily because the compact features in this source are all presumed to be of very small angular extent. The situation with the compact masers in Arp 220 is, however, quite different in that the structures span a range of scale sizes, and there are clearly coherent structures of order 10pc in extent (Lonsdale *et al.* 1998), suggesting that there are coherent physical associations of OH gas on these scale sizes.

Clearly, new observational constraints on the nature of the OH masing medium are needed. We describe observations of maser amplification and OH absorption of unresolved, sub-parsec-scale RSN continuum sources. These data constitute a probe of the OH gas along a very narrow, highly specific line of sight between us and the RSN, and as such allow us to dissect the OH-bearing medium with far greater precision than has hitherto been possible.

## 2. Observations and results

We observed Arp 220 on 9 November 2003 and 6 March, 2005 with an array comprising the 10 VLBA antennas, the phased VLA, the GBT, Arecibo, and 5 antennas of the European VLBI Network (EVN). Due to interference problems, data from the phased VLA had to be discarded.

Each observation covered a period of almost 21 hours. The dual-polarization spectral-line data spanned 8 MHz centered at 1637 MHz, thereby covering the redshifted frequencies of both the 1665 MHz and 1667 MHz main OH lines, with sensitivity to departures from the systemic velocity of at least  $\pm 400 \text{ km s}^{-1}$ . The data were processed in the VLBA correlator in Socorro with 512 channels across the 8 MHz band, yielding 15.625 kHz spectral resolution ( $\sim 2.8 \text{ km s}^{-1}$  velocity resolution).

A continuum image and a spectral line image cube, with precise spatial alignment via phase referencing on a strong maser feature, were generated using the AIPS software package. Spectra were extracted from the cube at the locations of all 49 continuum point sources, and candidate spectral features were noted both in absorption and emission.

In order to develop confidence in candidate spectral features, we adopted a strategy of examining the degree to which the purported spectral feature was localized to, and thus presumed to be associated with, the continuum source. We examined spectra from locations immediately surrounding the continuum source, in order to verify that all such locations were consistent with the absence of spectral features of any kind, whether or not they match the properties of the candidate feature. We also constructed an image of the region surrounding the source, integrated over the spectral range of the candidate feature, in order to verify that a well-defined, unresolved peak (or hole in the case of absorption

features) was present at the target location. These tests guard against specific image pathologies in both position and frequency.

For candidate spectral features that displayed signal-free noise-like comparison spectra at surrounding locations, and which showed a well-defined unresolved peak in the integrated image, we deemed the detection secure.

Both emission and absorption features are easier to detect in association with the stronger continuum sources. The  $\sim 1\text{mJy}$  source W30 (Lonsdale *et al.* 2006) shows both types of spectral feature with high signal to noise ratio, and is shown in Figure 1 as an illustration of the phenomena under study. This particular source displays multiple velocity systems with strong maser emission in both 1665 MHz and 1667 MHz main lines of OH, broad emission line velocity widths, and a broad absorption trough.

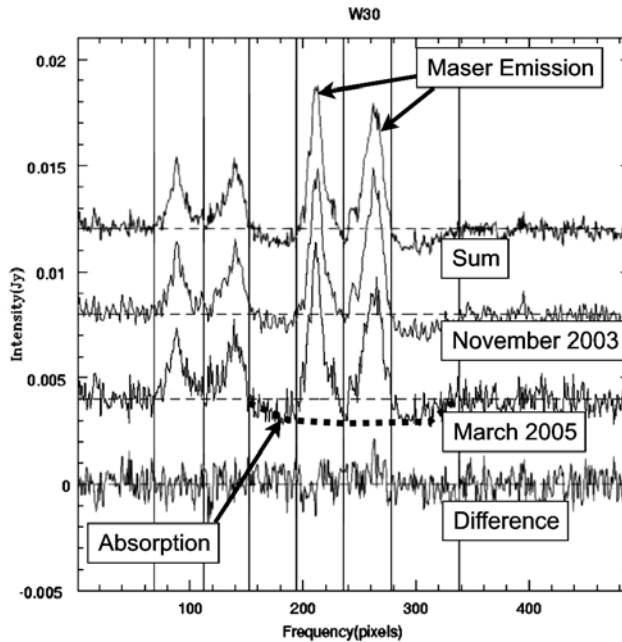


**Figure 1.** Spectra of the supernova-related continuum source W30 in Arp 220. The two center spectra are the two observing epochs, while the top and bottom spectra are the sum and difference respectively of the two epochs. The spectra have been offset vertically for clarity, and the horizontal dashed lines show the zero flux level for each spectrum. Each “pixel” on the frequency axis corresponds to 15.625 kHz, which is about 2.8 km/sec. The heavy dashed line shows an apparent, very broad absorption trough, several hundred km/sec wide. The vertical lines delineate subjectively separate features for feature verification and parameter extraction purposes. Two distinct velocity systems are present, in each of the main OH lines.

A total of 16 out of 49 supernova-related continuum point sources in Arp 220 have been found to exhibit detectable OH spectral features, and a total of  $\sim 30$  discrete spectral features have been identified, roughly 20 in emission and 10 in absorption. A handful of spectral features also exhibited strong variability between the two observing epochs. Typical inferred optical depths, both in emission and absorption, for the detected features are of order 1 or 2. Most of the 49 continuum sources are too weak to allow detection of absorption, and would require maser amplification factors of up to 100 to be detectable in OH emission. Therefore, the 30% detection rate should be regarded as a lower limit to the fraction of sources with OH optical depths in either emission or absorption found to be typical of the detected sources.

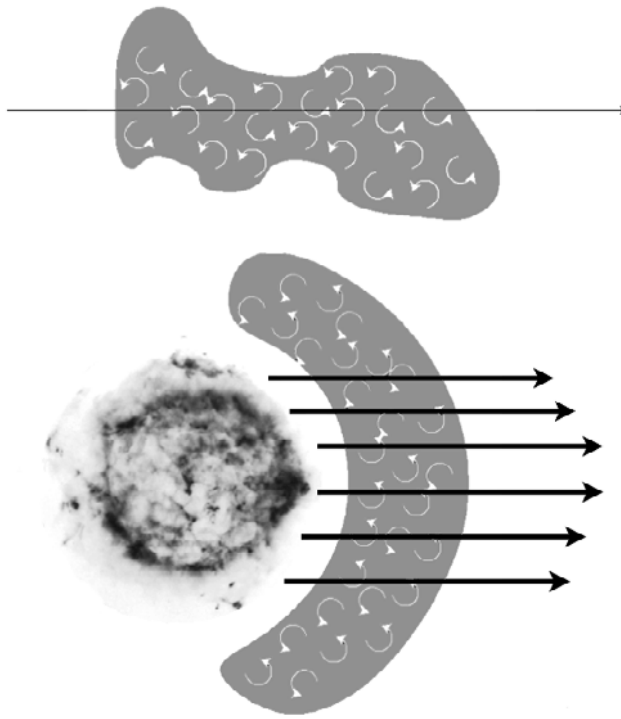


**Figure 2.** Illustration of two possibilities for generation of spectrally broad OH features associated with a physically compact continuum source. The upper cartoon shows a single, very narrow line of sight through a turbulent OH-bearing medium. The observed velocity width arises from the velocity dispersion along the line of sight. This picture implies that the particular lines of sight picked out by the supernova locations are not special, and that OH optical depths observed in association with the continuum sources are typical of all sight lines. The lower cartoon shows how a turbulent circumstellar OH-bearing medium might be sampled in many different locations by continuum emission from a synchrotron source (the RSN or SNR) extended on comparable scales. In this case the observed velocity width could arise from systematic velocity gradients within the OH-bearing shell, perhaps induced by the massive star progenitor or by the explosion itself.

### 3. Discussion and conclusions

The compact continuum sources in Arp 220 arise from starburst-related supernova activity, and are likely a mixture of radio supernovae (RSN) and young supernova remnants (SNR), the distinction being whether the ejected material from the explosion is still confined to the pre-existing progenitor stellar wind, or whether it has reached the undisturbed interstellar medium (Lonsdale *et al.* 2006, Parra *et al.* 2007). As such they are expected to be very compact, with linear extents ranging from a few light weeks for the youngest sources to perhaps as much as a parsec for the oldest remnants. Absorption or maser emission seen against these sources therefore represents sampling of a correspondingly narrow cylinder of material in the interstellar medium of Arp 220.

Given the extremely narrow cylinder being sampled, the observed velocity width of the spectral features is surprising, and implies either moderate velocity gradients along the line of sight, or extreme velocity gradients in the transverse direction. These possibilities are illustrated schematically in Figure 2.

In the scenario where the velocity gradients are longitudinal along the line of sight, the OH gas is necessarily distant from the associated supernova. This implies that the continuum supernova sources are randomly sampling the ISM of Arp 220, and that the amplification and absorption optical depths are typical for all sightlines in the region sampled by the supernovae. Consequently, all continuum emission in the region, whether supernova-related or not, should experience similar amplification and absorption, leading to predictable global OH line properties for Arp 220, given sufficient knowledge of the continuum emission distribution. The supernovae account for only a few percent of the total continuum emission in Arp 220. To the extent that discrete spectral features correspond to discrete OH-bearing clouds in the ISM, these observations can also yield constraints on the cloud parameters, in particular the internal velocity dispersion of the clouds. Further analysis may lead to useful constraints on the cloud overlap model described by Parra *et al.* (2005).

An interesting alternative explanation for the observed features is illustrated in the lower cartoon of Figure 2. It is plausible that the immediate vicinity of each supernova is an atypical environment in which OH emission and absorption is enhanced, most likely due to the disturbed circumstellar environment of the progenitor star. Conceivably, a shell of turbulent, OH-bearing gas exists which will be illuminated by the post-explosion synchrotron source. In this picture, strong velocity gradients may occur transversely across the continuum source, despite the small physical extent.

Distinguishing between these possibilities requires further work. It is worth noting, however, that line variability on  $\sim 1$  year timescales would be a natural consequence of the local shell scenario, because the line properties result from different lines of sight, and those lines of sight evolve on such timescales for sources of the observed age.

Further monitoring of the continuum sources and associated OH features in Arp 220 is ongoing.

## Acknowledgements

CJL acknowledges support from NSF grant AST-0352953 to the MIT Haystack Observatory. KdK acknowledges support through the REU program at Haystack Observatory, NSF grant AST-0138508.

## References

- Baan, W.A., Wood, P.A.D., & Haschick, A. D. 1982, *ApJ* 260, 49
- Diamond, P.J., Norris, R.P., Baan, W.A., Booth, R.S. 1989, *ApJ* (Letters) 340, L49
- Diamond, P.J., Lonsdale, Colin J., Lonsdale, Carol J., Smith, H.E. 1999, *ApJ* 511, 178
- Lonsdale, C.J., Diamond, P.J., Smith, H.E. & Lonsdale, C.J. 1998, *ApJ* (Letters) 493, L13
- Lonsdale, C.J., Diamond, P.J., Thrall, H., Lonsdale, C.J. & Smith, H.E. 2006, *ApJ*, 647, 185
- Parra, R., Conway, J.E., Elitzur, M. & Pihlstrom, Y.M. 2005, *A&A* 443, 383
- Parra, R., Conway, J.E., Diamond, P.J., Thrall, H., Lonsdale, Colin J., Lonsdale, Carol J. & Smith, H.E. 2007, *ApJ* 659, 314
- Pihlström, Y.M., Conway, J.E., Booth, R.S., Diamond, P.J., & Polatidis, A.G. 2001, *A&A* 377, 413
- Rovilos, E., Diamond, P.J., Lonsdale, C.J., Lonsdale, C.J. & Smith, H.E. 2003, *MNRAS* 342, 373
- Rovilos, E., Diamond, P.J., Lonsdale, C.J., Smith, H.E. & Lonsdale, C.J. 2005, *MNRAS* 359, 827
- Smith, H.E., Lonsdale, C.J., Lonsdale, C.J., & Diamond, P.J. 1998, *ApJ* (Letters) 493, L17